Proceedings of the World Congress on Engineering and Computer Science 2013 Vol I
WCECS 2013, 23-25 October, 2013, San Francisco, USA

Performance Improvement of a Diesel Generating Set with Fuzzy Control for Stand-alone and Grid-connected Operations

Giann B. Reis, Rodolpho V. A. Neves, Cassius R. Aguiar, Renan F. Bastos, Ricardo Q. Machado, and Vilma A. Oliveira

***Abstract*—This paper proposes a management strategy for a diesel generating set (GS) covering the mechanical part of the system which includes speed and active power control, the electrical part of the system which includes voltage and reactive power control, and the synchronism with the grid. The management is based on a fuzzy PD+I controller structure which uses a fixed controller surface for all fuzzy controllers (FCs). Simulations results for both stand-alone and grid-connected operations using fuzzy controllers were superior when compared to commercial methods (CM).**

***Index Terms*—Coordinated fuzzy control, Distributed generation, Gen-set, GS synchronism.**

I. Introduction

THE use of alternative energy sources in distributed generation (DG) systems improves voltage levels, reduces power losses in co-generation projects [1], and cuts power transmission costs as the DGs are installed close to the local consumption [2], [3], [4], [5]. Diesel-driven generators are commonly used due to their simplicity, wide range of power generation and low cost when compared to other alternative sources [2], [6], [7], [8].

One of the major problems caused by connecting a DG system to the grid is an alteration of the system-short-circuit parameters, which can lead to uncoordinated operation of the system protection and consequent damage to the electrical equipment connected to the DG terminals [9]. Unwanted oscillations in the power bus may also occur, as well as increased RI^2 and XI^2 losses in the impedance lines, caused by the reactive flow current [10]. One way to maintain the quality of the bus voltage within the established standards is to control the flow of active and reactive power of the connected DG.

Active power of the diesel GS can be controlled by regulating the torque provided by the diesel engine. On the other hand, reactive power of the GS is controlled by an automatic voltage regulator (AVR) which regulate the local bus voltage level and allows reactive power flow control [11].

The diesel GS is nonlinear [6], [12], due primarily to the torque-rotation ratio, actuators and motor valves. Fuzzy controllers have a good responses when used with nonlinear systems [13], [14], [15], [16], [17], [18], and have been used to regulate the grid-connected and stand-alone GS operation modes [3], [19], [20], [21], [22], [23], [24].

Manuscript received June 26, 2013. This paper was supported by Fundação de Amparo à Pesquisa do Estado de São Paulo under grant FAPESP-2011/02170-5.

G. B. Reis is with the Electrical Engineering Department, Engineering School of São Carlos, University of São Paulo - USP, SP - BRAZIL, e-mail: giann@sc.usp.br.

A fuzzy control approach for both stand-alone and grid-connected operations of the entire GS is proposed. The GS fuzzy controller designed for stand-alone operation is presented first, followed by the fuzzy approach for grid-connected operation in which the terminal voltage and reactive power controllers are coordinated to reduce the reactive power exchange with the IEEE Standard 1547 model grid.

II. System Description

The plant used in this study was built with PSCAD® software and comprises an IEEE-1547 standard grid, a DG system, control loops, transformers and local loads.

The DG used is a diesel GS which consists of a diesel engine (see block diagram in Fig. 1) and a synchronous generator. The motor input *Gate* is the output of the speed controller or the active power controller. The motor output is the torque which transfers the mechanical power from the diesel engine to the synchronous generator.

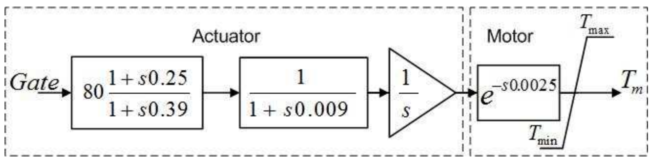

Fig. 1. Block diagram of the diesel engine model.

The synchronous generator used is represented by a standard synchronous machine model obtained from the PSCAD® software library configured with 1112 kVA and the parameters set according to 3512 model Caterpillar engine. This model is described in detail in [10].

The grid consists of a 100 MVA feeder built according to IEEE Std 1547.2 [25] operating at 69 kV.

The characteristics of dynamic loads have a substantial influence on the behavior of the GS. To analyze the transient behavior, the loads were dimensioned for an absorbed power around 20% of the nominal power of the GS. To represent some typical loads found in distribution networks, three loads having different dynamic responses were selected as follows:

1) a 215 HP induction machine set as 480 V and 140 A;
2) an RLC load whose power and passive elements are: R=1.536 Ω; L=3.950 mH; C=5.424 mF; P=154 kW and Q=149 $kVAr$; and
3) an uncontrolled rectifier feeding a resistance of 2.5 Ω – which consumes 250 kW.

ISBN: 978-988-19252-3-7
ISSN: 2078-0958 (Print); ISSN: 2078-0966 (Online)

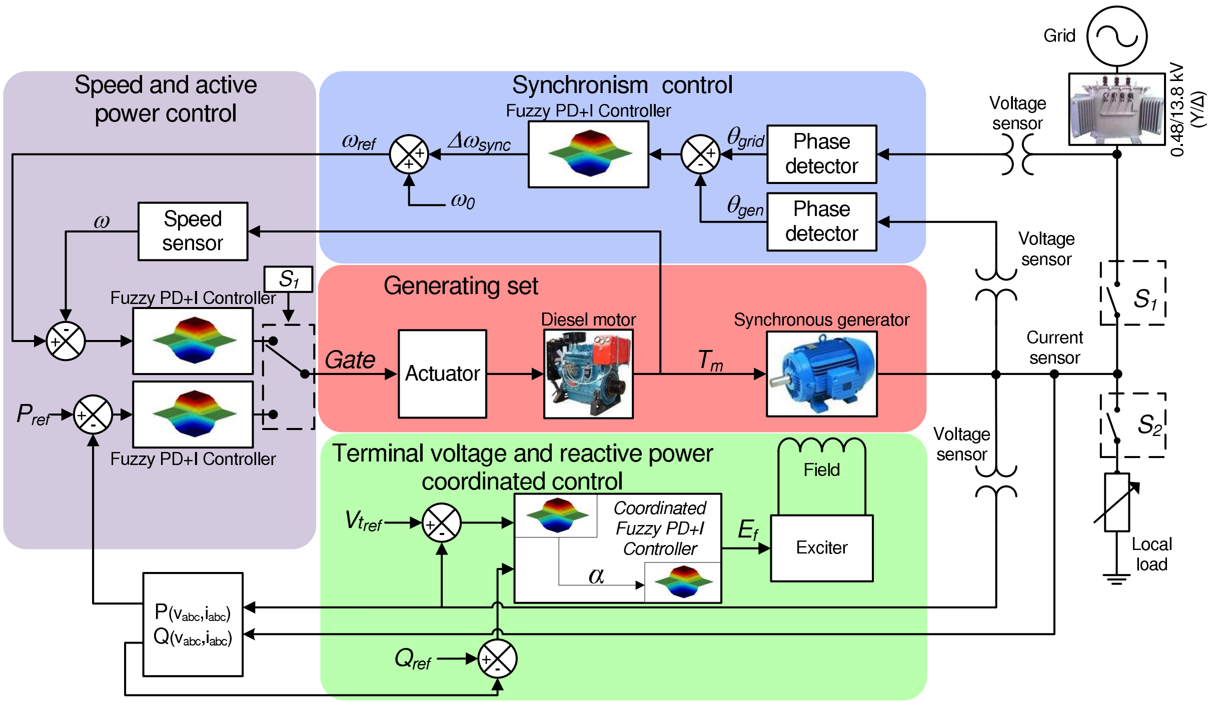

Fig. 2. GS block diagram showing the variables used by the controllers.

III. Control Strategy

A FC approach was used for each DG's control loop. The block diagram of the diesel GS with terminal voltage, speed, synchronism and power control loops is shown in Fig. 2, with the signal acquisition points used in the control loops and the block diagram of the FC in Fig. 3 with R the reference, y the variable measured, U the output, K_i the integrating gain of the error, K_p and K_d the normalizing gains for the inputs eP and eD, respectively.

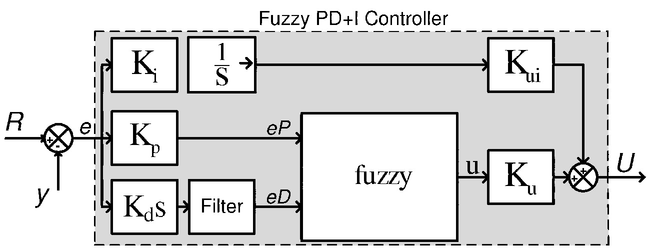

Fig. 3. Fuzzy PD+I controller.

Also, a low pass first order filter was used to eliminate the noise from the derivative term eD. The FC output gains K_{ui} and K_u were adjusted such that the controller output U belongs to the universe of discourse of the control variable, i.e., if the controller is for the motor speed the K_{ui} and K_u gains should be adjusted such that U corresponds to a torque belonging to the interval 0 to 1.1 pu.

The process of fuzzy inference follows a set of rules determined from expert knowledge and is typically based on the system's heuristic [19]. The fuzzy controller was derived from a control surface which represents the required nonlinearities such that fast actions on disturbances, but maintaining the damping required to stabilize the system, are taken.

The surface was defined by the membership functions shown in Fig. 4(a), as well as fuzzy rules and output functions formed by singletons as presented in Fig. 4(b).

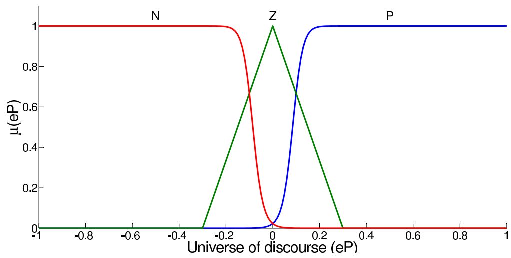

(a)

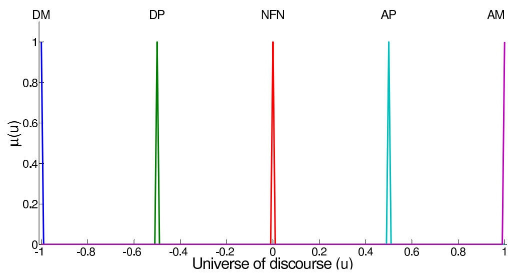

(b)

Fig. 4. Membership functions of inputs and output. In (a), the functions "P" and "N" have bell distributions and "Z" is triangular; in (b), the functions "DM", "DP", "NFN", "AP" and "AM" are singletons.

The use of singletons as output membership functions makes simpler the computations and allows the control output to be driven to its extreme values, whereas the use of triangular and bell distributions as input membership functions introduces nonlinearities in the control output such that fast and efficient responses are obtained [26]. The bell membership functions give fast responses to correct transitory disturbances while the triangular membership functions limitate the controller action on steady-state error.

The rules of inference comprise linguistic expressions such as "If eP is P and eD is Z then u is AP" and combine all inputs to provide a particular output. Table 1 shows the combinations of the two inputs and one output of the fuzzy system.

TABLE I
FUZZY SYSTEM INFERENCE RULES

		eP		
		N	Z	P
eD	N	DM	DP	NFN
	Z	DP	NFN	AP
	P	NFN	AP	AM

To implement the controller, the crisp output is obtained by the center of area defuzzification method [13], which yields

$$u = \frac{\sum_{k=1}^{N} \mu(V_k)V_k}{\sum_{k=1}^{N} \mu(V_k)} \tag{1}$$

where N is the number of discretization points of the universe of discourse for the output, μ is the degree of truth and V_k is the crisp value which the fuzzy system returns for each input set.

The control surface obtained from the fuzzy rules and membership functions presented in this paper is shown in Fig. 5. The surface shows abrupt variations at the border between positive and negative values such that fuzzy outputs with the same feature are provided, i.e., the fuzzy controller output changes faster when the inputs cross zero. The lateral plateaus show that when the inputs have opposite signs, the fuzzy controller output should be zero. In this case, the system tends to reach the equilibrium point then no action is needed. On the other hand, for situations in which both inputs are positive or negative, the fuzzy controller tends to saturate at its maximum or minimum points, and consequently the fuzzy controller should take more drastic actions for the system to return to its equilibrium point.

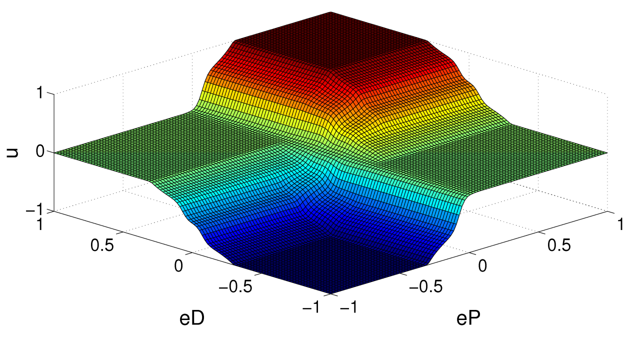

Fig. 5. Fuzzy control surface.

A. Speed and Active Power Control

The command switch S_1 shown in Fig. 2 selects the GS operation mode. When the GS is under stand-alone operation mode, the switch S_1 sets the speed control loop as active. Otherwise, the active power control is set as active. Fig. 6 shows the speed and active control loops along with the synchronism loop.

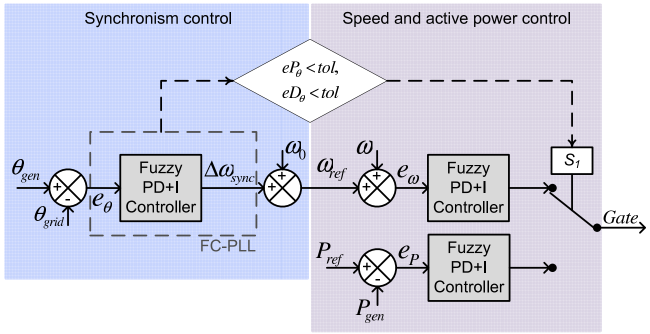

Fig. 6. Control scheme for active power, speed and synchronism.

The fuel valve aperture *Gate* is used to regulate the diesel motor speed when the DG operates disconnected from the grid. The signal frequency generated at the synchronous machine terminals is a function of the motor speed due to the coupling between the shaft of the generator and the diesel engine [27]. However, when the DG is connected to the grid, the coupling produces the active power delivered to the grid, since in this case the frequency is determined by the grid.

The input of the speed fuzzy controller is the error signal given by:

$$e_\omega = \omega_{ref} - \omega \tag{2}$$

where ω is the speed measured from the GS shaft and ω_{ref} is the speed reference that is constantly adjusted while the GS is disconnected according to

$$\omega_{ref} = \omega_0 + \Delta\omega_{sync} \tag{3}$$

where ω_0 is the rated synchronous speed and $\Delta\omega_{sync}$ is the output of the synchronism controller.

The diesel engine accelerates or decelerates to synchronize and connect the GS to the grid. The synchronism controller uses the difference between θ_{grid} and θ_{gen} and produces the deviation $\Delta\omega_{sync}$.

The generator voltage $V_{t_{gen}}$ must be synchronized with the reference obtained from the grid to enable the GS connection to grid.

The synchronism CM is performed by tracking the phases of the grid and DG voltages to connect the DG system at the time that the difference between the phases is within a preset tolerance.

However, there are active and reactive power disturbances during the DG connection before the synchronism is established. To reduce these disturbances, a fuzzy controller phase-locked loop (FC-PLL) shown in Fig. 6 is used. Using a phase detector, the argument θ is extracted from the DG and grid voltages θ_{gen} and θ_{grid}, respectively. The input of the FC-PLL is the error e_θ between the phase signals from GS and the grid.

In the proposed FC-PLL, the GS connection occurs not only when the proportional error term eP_θ is within a given tolerance, which means $0 \leq eP_\theta \leq tol$, but also when the derivative error term eD_θ is within the given tolerance. At the moment eP_θ and eD_θ are within the given tolerance, the switch S_1 is triggered to change the GS operation mode to grid-connected and then the active power control is set as active. The FC-PLL uses eD_θ to modify the θ_{gen} speed to match with the θ_{grid} speed. Therefore, the FC-PLL reduces

ISBN: 978-988-19252-3-7
ISSN: 2078-0958 (Print); ISSN: 2078-0966 (Online)

the differences in phases and frequencies between the GS and grid voltages and allows the error to reach the established tolerance which minimizes the transient disturbances at the connection time.

The output of the FC-PLL yields the signal $\Delta\omega_{sync}$ which feeds the speed control loop of the GS and is responsible to change the speed reference ω_{ref} (Fig. 6). The reference speed is thus dependent on the $\Delta\omega_{sync}$ and consequently accelerates or decelerates the generated voltage until it is in synchronism with the grid voltage.

The instant that the DG is connected to the grid the speed control loop is switched off by S_1. The active power controller is then activated and takes over the operation of the diesel engine to follow the active power reference P_{ref}. The active power used to control the power supplied to the grid is given by power average calculated by:

$$P_{gen} = \frac{1}{T} \int_0^T p \; dt. \tag{4}$$

B. Coordinated Control of the Terminal Voltage and Reactive Power

The approach presented for voltage and reactive power regulation differs from the AVRs available on the market, as it uses two fuzzy loops in parallel to control the voltage and reactive power supplied by the generator.

Reactive power and voltage amplitude are regulated by the synchronous generator field voltage (E_f). Unlike existing commercial systems loops where the voltage and reactive power control operate independently in the synchronous generator, the proposed approach uses two interconnected fuzzy control loops whose responses work together to regulate the generator exciter, as illustrated in Fig. 7. In Fig. 7, the upper loop regulates the terminal voltage to follow $V_{t_{ref}}$ set to 1 p.u. The lower loop regulates the reactive power according to the set point Q_{load}, the reactive power average measured from the local load. Therefore, the set point was adjusted to supply the local load and the reference value changes accordingly to the reactive power demanded by the load, i.e., if there is no reactive power load, Q_{load} is set to 0 kVAr.

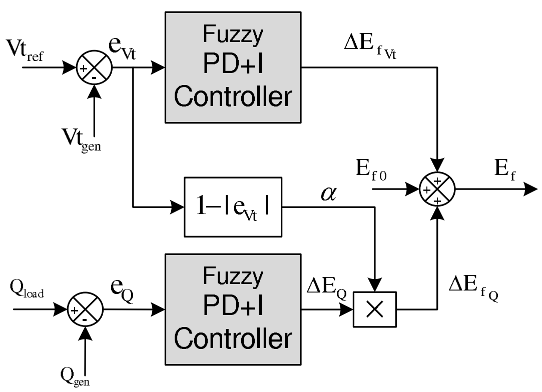

Fig. 7. Configuration of the coordinated fuzzy PD+I controller for terminal voltage and reactive power.

Therefore, the GS supplies only the reactive power needed for these loads, and cancels the reactive power exchange between the DG and the grid, which favors the maintenance of the unity power factor at the point of the DG connection. The average reactive power can be calculated by:

$$Q_{gen} \;\; = \;\; \frac{1}{T} \int_0^T q \; dt \tag{5}$$

with q the instantaneous reactive power.

The excitation voltage field E_f is obtained by adding the three terms:

$$E_f = E_{f_0} + \Delta E_{f_{V_t}} + \Delta E_{f_Q} \tag{6}$$

with E_{f_0} the initial condition of the field, $\Delta E_{f_{V_t}}$ the term given by the voltage controller and ΔE_{f_Q} the term given by the reactive power controller. The term ΔE_{f_Q} is given by:

$$\Delta E_{f_Q} = \alpha \; \Delta E_Q \tag{7}$$

where α is a weighting factor given by:

$$\alpha = 1 - |e_{V_t}| \tag{8}$$

which has maximum value when e_{V_t} is zero. This strategy thus ensures effective reactive power control as the error voltage decreases by prioritizing the terminal voltage control, and it also avoids large oscillations in the voltage level supplied to the load, which improves the GS power quality.

IV. Simulation Results

The stand-alone operation mode test was performed with connection and disconnection of loads. The simulation of the grid-connected operation mode was performed after the connection of the GS to the grid using the FC-PLL. Moreover, the simulation considered active power injection into the grid by the DG system. Results using existing CM and controllers are presented for comparison purposes.

Fig. 8(a) demonstrates that when the synchronism CM is used with a phase error tolerance of $0.5°$, large variations in P and Q, of 250 kW and 90 kVAr, respectively, are observed, what represent 22.5% and 8.1% of the GS nominal power. However, with the FC-PLL there is a small variation in P. It is also noticed a 8 kVAr peak variation in Q, i.e., 0.7%, of the GS nominal power whereas with the CM the variation in Q is about 8.1% as shown in Fig. 8(b).

The loads connection were conducted similarly for each GS operation mode. First, at $t = 10$ s, a 215 HP three-phase induction motor (IM) was connected (driven by an increased torque ramp until the torque reached 1 p.u.) and remained connected for 10 s until it was disconnected. An RLC load was then connected at $t = 25$ s up to 35 s. Finally, a three-phase uncontrolled rectifier was connected to the grid at $t = 40$ s up to $t = 50$ s.

The results presented in Fig. 9 show the action of the speed and terminal voltage controllers for the stand-alone operation mode. One simulation used the FC for the speed and voltage terminal, whereas another used a commercial controller for speed (CC_ω) from the PSCAD® library with the parameters given in Table II and a Proportional-Integral controller (PI) set according to [28] to regulate the terminal voltage.

Compared with the proposed FC, the PI associated with the CC_ω (CC_ω+PI) allowed speed variations 2.5 times greater when connecting or disconnecting loads which exceeded the

ISBN: 978-988-19252-3-7
ISSN: 2078-0958 (Print); ISSN: 2078-0966 (Online)

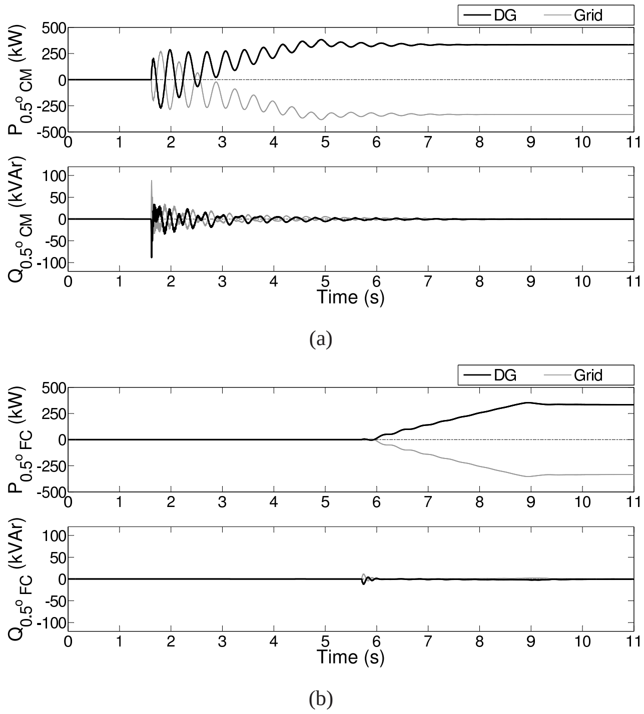

(a)

(b)

Fig. 8. Transients in P and Q caused by the effect of the grid connection. Where (a) is for CM and (b) is for FC-PLL.

limit recommended by IEEE Std 1547.2 [25] as shown in Fig. 9 by UsL limit, and also presented responses which were twice slower. Results for the terminal voltage were similar for both controllers.

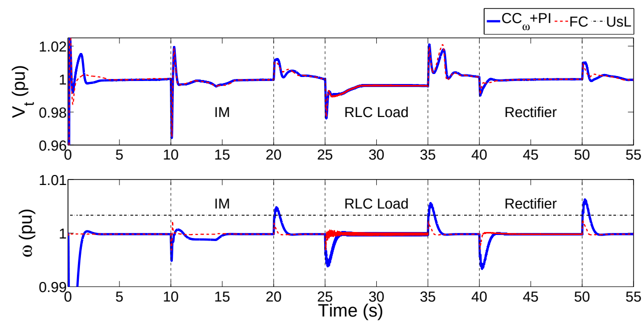

Fig. 9. GS terminal voltage and speed obtained with the FC and CC_ω+PI controllers with the recommended UsL for the stand-alone operation mode.

The load tests for grid-connected operation mode followed the same steps previously described for evaluating the controllers with the GS disconnected. Figs. 10 and 11 compare, respectively, the results obtained for the P and Q powers by the FC developed with those from the GS controlled by a PI for the exciter set according to IEEE Std 421 [29], and a commercial controller for active power control (CC_P) with parameters given in Table II. Results are obtained for power transference and load connections using the association of the CC_P and PI (CC_P + PI) and the proposed FC.

TABLE II
COMMERCIAL CONTROLLERS

Speed $CC_\omega(s)$	Active power $CC_P(s)$
$\frac{0.0625s+0.25}{0.0002s^2+0.001s+1}$	$\frac{0.00125s+0.005}{0.0002s^2+0.001s+1}$

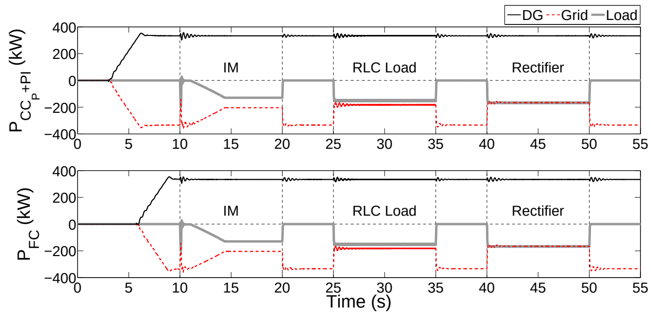

Fig. 10. Active power generated and absorbed by the elements that comprise the system.

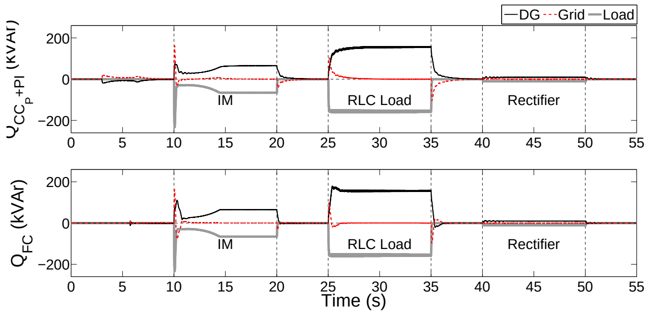

Fig. 11. Reactive power generated and absorbed by the elements that comprise the system.

The P and Q power responses are positive when the source provides energy, otherwise it consumes energy. Variations in Q were ten times smaller at the connection time of the GS to the grid and responses twice faster to stabilize Q at the connection of loads using the proposed FC when compared to the commercial controllers.

The terminal voltage response was also faster with the FC than with the PI as shown in Fig. 12.

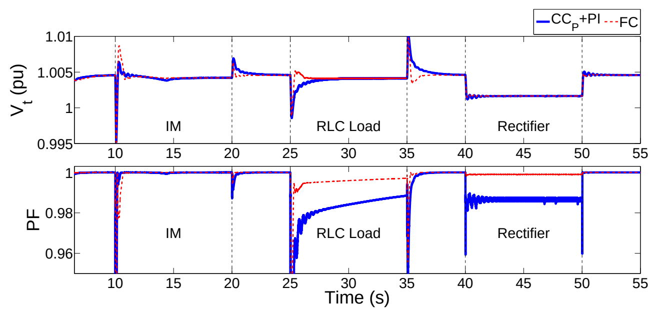

Fig. 12. Comparison of the terminal voltage and power factor for the $CC_P + PI$ and FC.

The root mean square errors of the power factor deviation from the unity were 1.695% for the association CC_P+PI and 1.228% for the proposed FC, demonstrating that the FC was faster in correcting the terminal voltage.

V. CONCLUSION

The management proposed was efficient to control the diesel engine and the synchronous machine and also the synchronism with the grid. The proposed controllers also allowed fast and accurate actions, leading to smaller oscillations of the controlled variables in relation to a commercial controller.

The FC coordinated structure developed was able to regulate the reactive power generated to increase the power factor at the point of connection to the distribution grid, while maintaining the level of the terminal voltage within the limits recommended by IEEE Std 1547.2 [25]. Thus, the coordinated FC with reactive power control showed to be efficient to supply the local loads with the reactive power coming from the GS and avoiding reactive power exchanges with the grid.

The FC-PLL reduced the transient caused by the connection to the grid as recommended by IEEE Std 1547.2 [25], which avoided the propagation of the active power transfer disturbance to the grid. With the synchronism CM the disturbance was significant, extending over the entire period of power transfer increasing.

Although the synchronism CM provides a faster connection between the sources, it allows large disturbances in P and Q since there is only phase control. However, the FC-PLL was able to reduce the phase difference and also adjusted the speed which the phase difference was reduced.

The grid-connected FC enabled a power factor closer to unity for the different simulation scenarios, whereas the commercial controllers showed a similar PF and V_t responses only for the IM connection which absorbs power slowly.

REFERENCES

[1] W. Elkhattam and M. Salama, "Distributed generation technologies, definitions and benefits," *Electric Power Systems Research*, vol. 71, no. 2, pp. 119–128, Oct. 2004.

[2] M. Rashed, A. Elmitwally, and S. Kaddah, "New control approach for a pv-diesel autonomous power system," *Electric Power Systems Research*, vol. 78, no. 6, pp. 949–956, Jun. 2008.

[3] N. Sisworahardjo, M. El-Sharkh, and M. Alam, "Neural network controller for microturbine power plants," *Electric Power Systems Research*, vol. 78, no. 8, pp. 1378–1384, Aug. 2008.

[4] A. Amr, S. Rady, and E. Badreddin, "A plant for cogeneration of electricity and water powered by renewable energy sources based on using high level of automation," in *Proc. 10th International Conference on Intelligent Systems Design and Applications (ISDA), 2010*, Cairo, Dec. 2010, pp. 209–213.

[5] P. Ray, S. Mohanty, and N. Kishor, "Dynamic modeling and control of renewable energy based hybrid system for large band wind speed variation," in *Proc. IEEE PES Innovative Smart Grid Technologies Conference Europe (ISGT Europe), 2010*, Gothenburg, Oct. 2010, pp. 1–6.

[6] A. Cooper, D. Morrow, and K. Chambers, "Development of a diesel generating set model for large voltage and frequency transients," in *Proc. IEEE Power and Energy Society General Meeting, 2010*, Minneapolis, Jul. 2010, pp. 1–7.

[7] K. Pandiaraj, B. Fox, D. Morrow, S. Persaud, and J. Martin, "Centralised control of diesel gen-sets for peak shaving and system support," *IEE Proceedings - Generation, Transmission and Distribution*, vol. 149, no. 2, pp. 126–132, Mar. 2002.

[8] M. Kanoglu, S. K. Isik, and A. Abusoglu, "Performance characteristics of a diesel engine power plant," *Energy Conversion and Management*, vol. 46, no. 11–12, pp. 1692–1702, 2005.

[9] S. Chaitusaney and A. Yokoyama, "Impact of protection coordination on sizes of several distributed generation sources," in *Proc. The 7th International Power Engineering Conference, 2005. IPEC 2005*, vol. 2, Singapore, Dec. 2005, pp. 669–674.

[10] P. Kundur, *Power System Stability and Control*. New York: McGraw-Hill, 1994.

[11] S. Vachirasricirikul, I. Ngamroo, and S. Kaitwanidvilai, "Coordinated SVC and AVR for robust voltage control in a hybrid wind-diesel system," *Energy Conversion and Management*, vol. 51, no. 12, pp. 2383–2393, 2010.

[12] A. Cooper, D. Morrow, and K. Chambers, "A turbocharged diesel generator set model," in *Proc. 44th International Universities Power Engineering Conference (UPEC), 2009*, Glasgow, Sep. 2009, pp. 1–5.

[13] W. Chen, L. Jiao, R. Li, and J. Li, "Adaptive backstepping fuzzy control for nonlinearly parameterized systems with periodic disturbances," *IEEE Transactions on Fuzzy Systems*, vol. 18, no. 4, pp. 674–685, Aug. 2010.

[14] H. Lee, "Robust adaptive fuzzy control by backstepping for a class of mimo nonlinear systems," *IEEE Transactions on Fuzzy Systems*, vol. 19, no. 2, pp. 265–275, Apr. 2011.

[15] S. Islam and P. Liu, "Robust adaptive fuzzy output feedback control system for robot manipulators," *IEEE/ASME Transactions on Mechatronics*, vol. 16, no. 2, pp. 288–296, Apr. 2011.

[16] K. Tanaka, M. Tanaka, H. Ohtake, and H. Wang, "Shared nonlinear control in wireless-based remote stabilization: A theoretical approach," *IEEE/ASME Transactions on Mechatronics*, vol. 17, no. 3, pp. 443–453, Jun. 2012.

[17] T. Tong and Y. Li, "Adaptive fuzzy output feedback tracking backstepping control of strict-feedback nonlinear systems with unknown dead zones," *IEEE Transactions on Fuzzy Systems*, vol. 20, no. 1, pp. 168–180, Feb. 2012.

[18] H. Wu, J. Wang, and H. Li, "Exponential stabilization for a class of nonlinear parabolic pde systems via fuzzy control approach," *IEEE Transactions on Fuzzy Systems*, vol. 20, no. 2, pp. 318–329, Apr. 2012.

[19] D. McGowan, D. Morrow, and B. Fox, "Multiple input governor control for a diesel generating set," *IEEE Transactions on Energy Conversion*, vol. 23, no. 3, pp. 851–859, Sep. 2008.

[20] C. Su, H. Hwung, and G. Lii, "Fuzzy logic based voltage control for a synchronous generator," *Electric Power Systems Research*, vol. 41, pp. 225–231, 1997.

[21] R. Liang and Y. Wang, "Fuzzy-based reactive power and voltage control in a distribution system," *IEEE Power Engineering Review*, vol. 22, no. 12, pp. 610–618, Dec. 2002.

[22] M. Moutinho, C. da Costa, W. Barra, and J. Barreiros, "Identification, digital control and fuzzy logic techniques applied to a synchronous generator," *IEEE Latin America Transactions*, vol. 7, no. 2, pp. 141–150, Jun. 2009.

[23] D. Gaonkar and G. Pillai, "Fuzzy logic based coordinated voltage regulation method for distribution system with multiple synchronous generators," in *Proc. 2010 IEEE PES Transmission and Distribution Conference and Exposition*, New Delhi, Apr. 2010, pp. 1–5.

[24] A. Soundarrajan and S. Sumathi, "Fuzzy-based intelligent controller for power generating systems," *Journal of Vibration and Control*, vol. 17, no. 8, pp. 1265–1278, 2011.

[25] IEEE Std 1547.2, "IEEE application guide for IEEE Std 1547, IEEE standard for interconnecting distributed resources with electric power systems," pp. 1–207, Apr. 2009.

[26] J. Jantzen, *Foundations of Fuzzy Control*. Chichester: John Wiley & Sons, Ltd., 2007.

[27] K. Cheong, P. Li, and J. Xia, "Control oriented modeling and system identification of a diesel generator set (genset)," in *Proc. American Control Conference (ACC), 2010*, Baltimore, Jul. 2010, pp. 950–955.

[28] D. Mota and C. Goldemberg, "Comparison between voltage control structures of synchronous machines," *IEEE Latin America Transactions*, vol. 8, no. 6, pp. 631–636, Dec. 2010.

[29] IEEE Std 421.5, "Approved IEEE recommended practice for excitation systems for power stability studies (superseded by 421.5-2005)," Feb. 2005.

ISBN: 978-988-19252-3-7
ISSN: 2078-0958 (Print); ISSN: 2078-0966 (Online)